JMEPEG (2022) 31:2708–2714
https://doi.org/10.1007/s11665-021-06342-7

1059-9495/$19.00

Effects of Different Cathodic Reactions on Tribocorrosion Behavior of AISI 430 in 0.5 mol/L Sulfuric Acid

Zhixin Dai, Ming Liu, Shengli Jiang, Mingyang Li, Shu Li, and Deli Duan

Submitted: 1 June 2021 / Revised: 28 September 2021 / Accepted: 2 October 2021 / Published online: 18 January 2022

It's well known that wear can accelerate degeneration of materials in corrosive media. Less attention has been paid to effects of different cathodic reactions on tribocorrosion behaviors. In this study, linear reciprocating sliding wear test of AISI 430 was carried out in distilled water and 0.5 mol/L sulfuric acid media, respectively. The results revealed that oxygen reduction reaction is in favor of oxide films forming on the surface, which increased subsurface hardness of the wear track. However, hydrogen evolution reaction restrained the formation of oxide films and induced hydrogen embrittlement, thus worsened the tribocorrosion properties and increased material removal. Interaction between wear and corrosion contributed most mass loss in the material deterioration, which was related to the reciprocating frequency.

Keywords AISI 430, cathodic reactions, oxide films, sulfuric acid, tribocorrosion

1. Introduction

For engineering materials, wear often occurs along with chemical or electrochemical reaction in service condition. This kind of wear is often referred to as tribocorrosion (Ref 1), which often happens in the marine environment, petrochemical industry, body fluid environment, and so on. Material degradation due to tribocorrosion, i.e, the synergism between wear and corrosion, which is more serious than single failure form, results in significant financial loss to production and living (Ref 2, 3). In fact, tribocorrosion doesn't mean simple sum of mechanical wear and chemical or electrochemical corrosion. The interaction plays an important role in this condition, which can significant increase the mass loss of materials, especially in ion solutions. For example, titanium alloys, aluminum alloys and stainless steels show good corrosion resistance in most environments due to formation of passive films. While in tribocorrosion condition, the mechanical action of wear can remove the passive films and accelerate the corrosion. Meanwhile, the mechanical property degradation caused by corrosion facilitates wear (Ref 4-6). Nowadays, more and more researchers are interested in the tribocorrosion issue. The total mass loss (W) caused by tribocorrosion can be separated into net wear component (W_{wear}), net corrosion component (W_{corr}) and their interactions (ΔW) (Ref 7).

It's well known that stainless steels are significant to us because of their plenitude of applications in our daily life, such as appliance industry, chemical industry, medical equipment, aerospace, etc., (Ref 8). For widely use of stainless steel, the most important property is its good corrosion resistance, which is primarily attributable to its chromium content. On the basis of Tammann's Law (Ref 9), Cr content (wt.%) of stainless steel is more than 11.7% and it reacts with oxidant to form a thin, chromium-rich passive film over the surface which provides the resistance to corrosion (Ref 10). Ferritic, austenitic and martensitic with precipitates, are main microstructures in stainless steel, which can be obtained by adjusting chemical compositions and heat treatment (Ref 8, 11). Accordingly, stainless steel can be categorized into ferritic stainless steels, austenitic stainless steels, martensitic stainless steels, duplex stainless steels, precipitation hardening stainless steels. With good behaviors in thermal conductivity, stress corrosion resistance, low tendency in work hardening and low cost, ferritic stainless steels get the second share of the market, especially in construction, transportation, and chemical industry.

AISI 430 is the typical kind of 17 percent Cr alloys ferritic stainless steels. The existing studies on tribocorrosion of AISI 430 are focused on its corrosion behaviors. The process and kinetics of corrosion, character and mechanism of electrochemistry, morphology and constituent of corrosion products have been studied intensively (Ref 12-15). The studies on wear are mostly focused on AISI 430 with surface modification, only a little work is related to tribocorrosion behaviors.

In ion solutions, the common cathodic reactions are hydrogen evolution reaction (HER), $H^+ + e^- \rightarrow H$, and oxygen reduction reaction (ORR), $\frac{1}{4}O_2 + \frac{1}{2}H_2O + e^- \rightarrow OH^-$. Therefore, it's significant to investigate the influence for different cathodic reactions on tribocorrosion behaviors of AISI 430.

Zhixin Dai, Ming Liu, Shengli Jiang, Shu Li, and **Deli Duan**, Shi-Changxu Innovation Center for Advanced Materials, Institute of Metal Research, Chinese Academy of Sciences, 72 Wenhua Road, Shenyang 110016, China; School of Materials Science and Engineering, University of Science and Technology of China, 72 Wenhua Road, Shenyang 110016, China; and Liaoning Key Laboratory of Aero-Engine Materials Tribology, Institute of Metal Research, Chinese Academy of Sciences, 72 Wenhua Road, Shenyang 110016, China; and **Mingyang Li**, Shi-Changxu Innovation Center for Advanced Materials, Institute of Metal Research, Chinese Academy of Sciences, 72 Wenhua Road, Shenyang 110016, China; and Liaoning Key Laboratory of Aero-Engine Materials Tribology, Institute of Metal Research, Chinese Academy of Sciences, 72 Wenhua Road, Shenyang 110016, China. Contact e-mails: sljiang@imr.ac.an and duandl@imr.ac.cn.

In this study, tribocorrosion behaviors of AISI 430 stainless steel in distilled water and 0.5 mol/L sulfuric acid media were systematically investigated and the interactions between mechanics and chemistry were discussed.

2. Experimental Material and Method

AISI430 stainless steel used in this study was hot-rolled and solution treated, XRF analysis were carried out and compositions are: C 0.035, Si 0.23, Mn 0.33, Cr 16.12, Ni 0.12, P 0.024, S 0.002, N 0.049, Fe balance. The microstructure is illustrated in Fig. 1. It shows that many second phases, maybe (Cr, Fe)7C3 (Ref 16, 17), are diffused inside ferrite grains and the boundaries.

The samples with the size of 10 × 10 × 3mm for potentiodynamic scanning were polished by 1200-grit silicon carbide paper and cleaned by ethanol. The exposed working area was 1 cm^2. All electrochemical measurements were performed with a standard three-electrode system. The counter electrode was a Pt sheet, and a saturated calomel electrode (SCE) with a Luggin capillary was used as the reference electrode. The tests were performed by using Gamry Interface 1000 electrochemical workstation at room temperature with distilled water and 0.5 mol/L sulfuric acid solutions. The pH of the acid solution is 0. The scanning rate of potentiodynamic scanning is 0.166 mV/s.

The samples with the size of 20 × 20 × 3 mm for tribocorrosion test were cleaned by ethanol, polished by 1200-grit silicon carbide paper and then polished by diamond paste (1.5 μm). The mass of the samples was measured before and after the experiment with an analytical balance. The tribocorrosion test was carried out with MFW-05 reciprocating tribotester in form of ball-on-flat (Ref 18). The counter pair were ϕ4mm Si_3N_4 ceramic balls. The applied loads were 30N, 60N, 90N, respectively. The reciprocating frequencies were 0.5, 1, and 2 Hz. The number of reciprocating sliding was 3600 with a single stroke of 10mm. The test media were distilled water and 0.5 mol/L sulfuric acid. The Leco LM 247 AT microhardness tester was used to measure the hardness of cross section of the samples from the worn surface to the base material.

3. Results and Discussions

3.1 Potentiodynamic Scanning Measurements for AISI 430 in Distilled Water and 0.5 mol/L Sulfuric Acid

The electrochemical polarization behavior of AISI 430 in distilled water and 0.5 mol/L sulfuric acid is illustrated in Fig. 2. E_{corr} and i_{corr} are illustrated in Table 1. The black curve in Fig. 2 reveals single corrosion potential, which means anodic current density is equal to the cathodic current density. This behavior is an indication of stable passive system and the Tafel slope is about $b_c \approx 160$ mV/dec. According to the mixed potential theory (Ref 19), the corrosion occurs at potential where the O_2 reduction rate, i_{O2}, is equal to the metal dissolution rate, i_{diss}. The measured current density, i_{net}, is the algebraic addition of i_{O2} and i_{diss}, .

In distilled water, the stainless steel can form passive film initiatively and be self-healing. The i_{corr} of AISI 430 is smaller than 5×10^{-7} A/cm^2. This result indicates that, in distilled water, the corrosion of metal can be ignored.

In 0.5 mol/L sulfuric acid, it reveals triple corrosion potentials $E_{corr\text{-}i}$, $E_{corr\text{-}ii}$, $E_{corr\text{-}iii}$, existed in the active, active-passive and passive regions, which means the system is in unstable passive state. Similar phenomenon was also found of high nitrogen bearing stainless steel in acidic chloride solution (Ref 20). At potential of $E_{corr\text{-}i}$, Tafel slope is about $b_c \approx 120$ mV/dec, according to this, the cathodic reaction is hydrogen evolution reaction, which gives a cathodic current. At $E_{corr\text{-}i}$, the cathodic current i_{H+} equals to anodic current i_{diss}. The measured current density, i_{net}, is the algebraic addition of i_{H+} and i_{diss}, .

In 0.5mol/L sulfuric acid, corrosion of AISI 430 occurs at $E_{corr\text{-}i}$, the protective passive film dissolves and i_{corr} enlarges observably, relative to which in distilled water. The i_{corr} of AISI 430 is about 2.48×10^{-4} A/cm^2. At potential between $E_{corr\text{-}i}$ and $E_{corr\text{-}iii}$, the cathodic current is smaller than anodic current

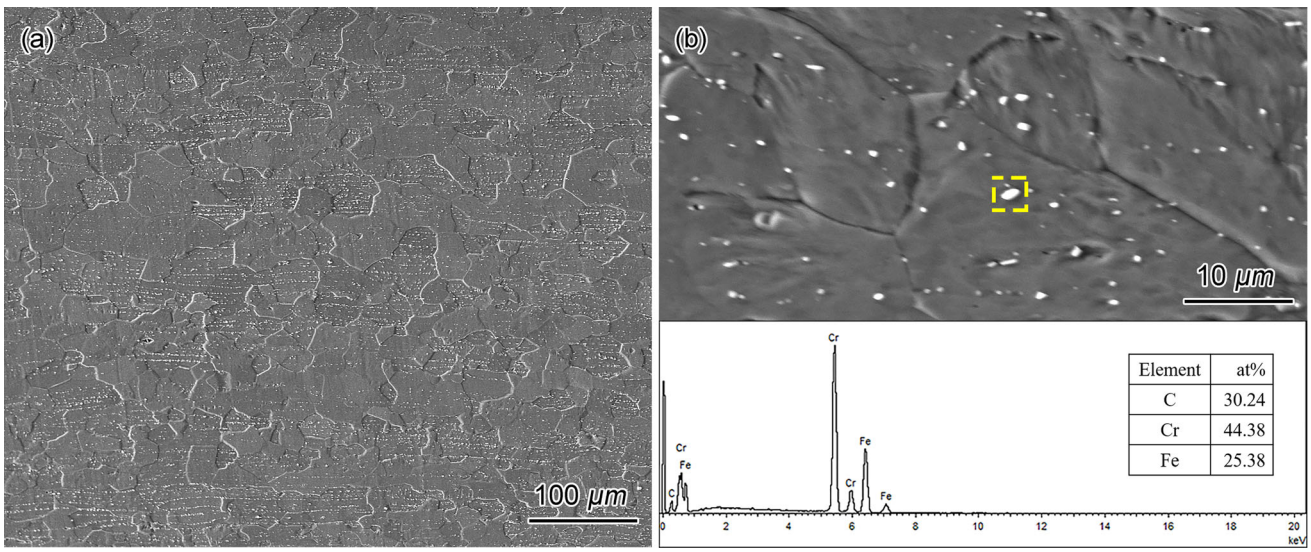

Fig. 1 Microstructure of (a) AISI 430 stainless steel and (b) second phase

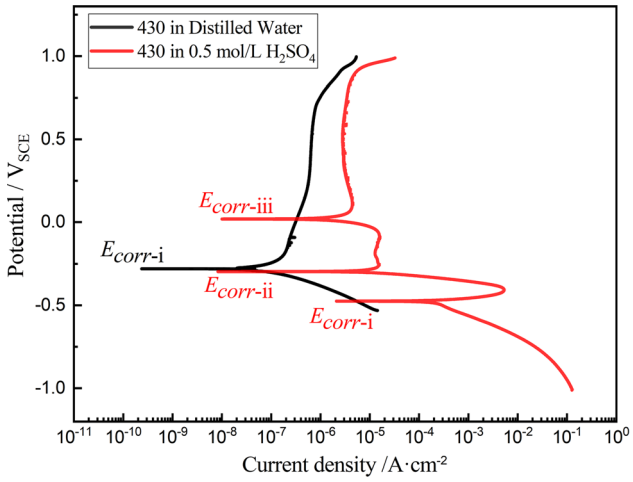

Fig. 2 Potentiodynamic polarization curves of AISI 430 stainless steel in distilled water and 0.5 mol/L H_2SO_4

Table 1 E_{corr} and i_{corr} values of AISI 430 stainless steel in different media

Experimental medium	$E_{corr\text{-}I}$, V_{SCE}	$i_{corr\text{-}I}$, A cm^{-2}
Distilled water	− 0.277	2.118×10^{-7}
0.5 mol/L·H_2SO_4	− 0.475	1.613×10^{-4}

and net current performs as anodic current. In active-passive transition, current decreases substantially and it becomes cathodic in potential between $E_{corr\text{-}ii}$ and $E_{corr\text{-}iii}$. This behavior has been ascribed as the rate of HER on the passive film greater than passive film dissolution (Ref 21). Above the third mixed potential ($E_{corr\text{-}iii}$), the net current performs as anodic current again.

3.2 Tribocorrosion Tests for AISI 430 in Distilled Water and 0.5 mol/L Sulfuric Acid

The coefficient of friction (COF) of tribocorrosion test is illustrated in Fig. 3. After 1200 cycles, the COF becomes stable. It can be seen clearly that the COF in 0.5 mol/L sulfuric acid is smaller than in distilled water. Due to the depolarization of H^+, oxidation film dissolves faster, compared with its formation, which can resist the adhesion grind against Si_3N_4. Furthermore, the positively charged surface formed on the samples by adsorption of the hydrogen ions brought the electrical double layer effect and the hydration effect (Ref 20), thus the COF of AISI 430 in 0.5 mol/L sulfuric acid is lower than that in distilled water.

However, lower COF doesn't mean lower mass loss. Figure 4 shows that AISI 430 has the much higher mass loss in sulfuric acid medium, while the corresponding COF is around 0.4 which is much lower than that in distilled water. For different frequencies, when the wear trip is fixed as 72 m, the testing duration is different. Lower frequency means more testing duration, which results in increasing of mass loss caused by corrosion. This phenomenon is much obvious in 0.5 mol/L sulfuric acid medium because of the high corrosion rate. Relatively, in distilled water, the corrosion rate of AISI 430 is much lower than that in 0.5 mol/L sulfuric acid. So, frequency

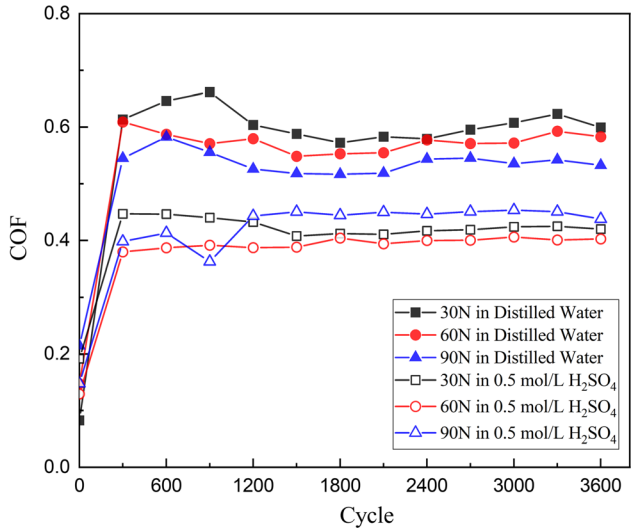

Fig. 3 COF of AISI 430 stainless steel in frequency 1Hz

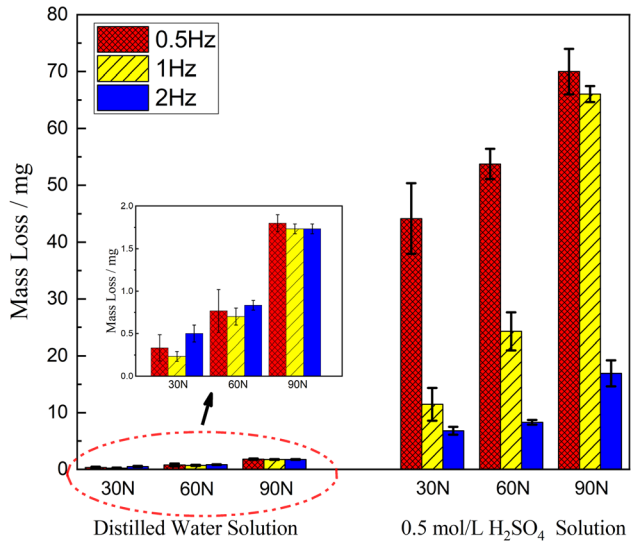

Fig. 4 Mass loss of AISI 430 stainless steel in different test conditions

has little influence in mass loss. The wear loss increased with loading both in sulfuric acid medium and distilled water, which indicates higher applied load causes more mass loss and higher deformation of materials.

The morphologies and EDS analyses of the worn surface are illustrated in Fig. 5. The wear tracks appear scratches and grooves, which is characteristic of abrasive wear. In distilled water, the worn surface is covered by oxide layer containing mainly Cr and Fe oxide with small amount of Si oxide. It was reported that above pH 3.5, under tribochemical conditions, Si_3N_4 can react with H_2O and form $SiO_2 \cdot nH_2O$ (Ref 22, 23). The surface is covered by oxidation film, which performs as protective layer and resist mass loss. With the applied load of 30 N, the oxide layer is discontinuous and the substrate exposes partly. With the increase in applied load, oxidation reaction induced by friction becomes more vigorous. In the condition of 60N, the oxide layer covered the surface completely. When the

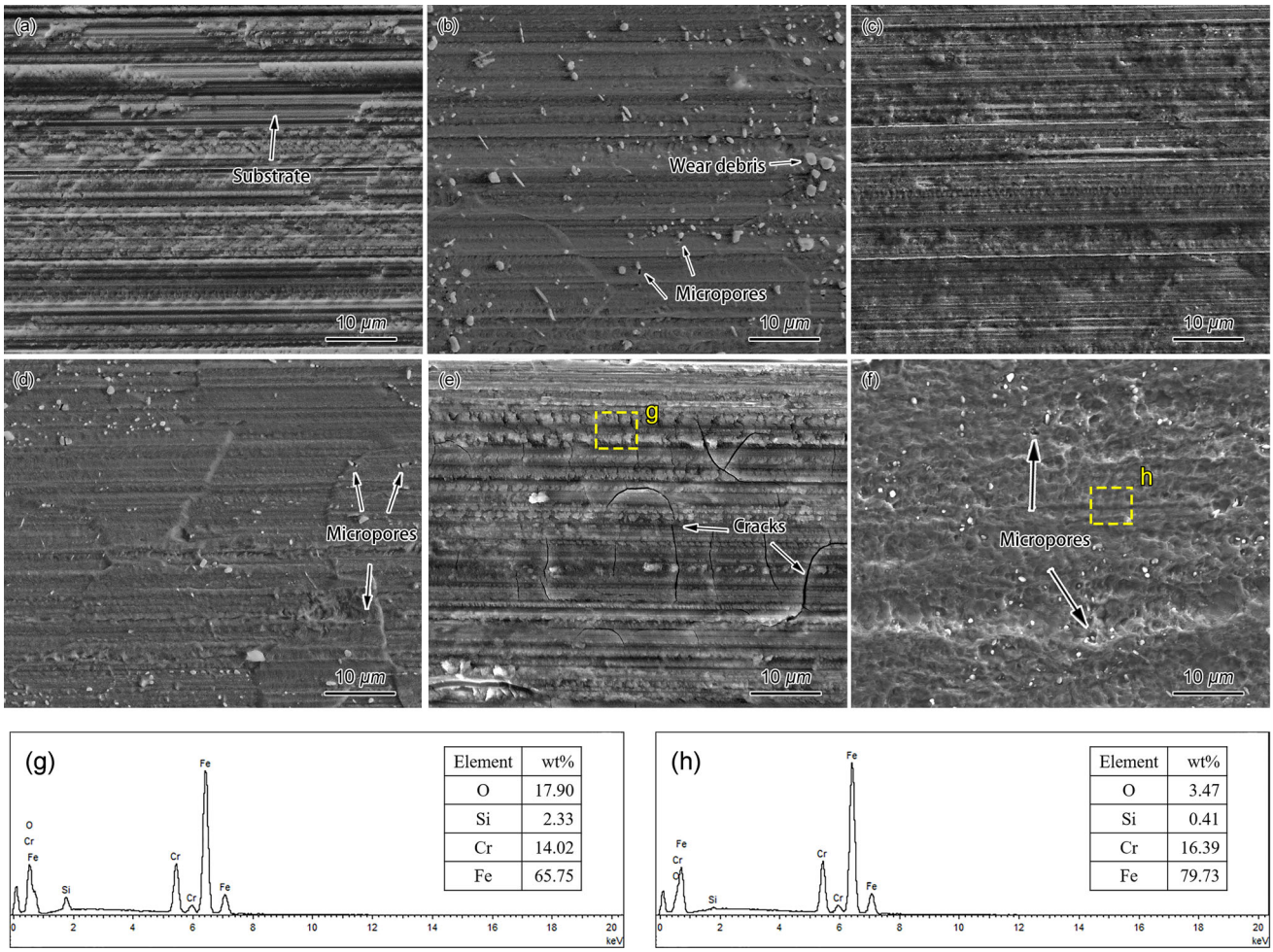

Fig. 5 Surface microstructures of AISI 430 stainless steel with applied load, (a) 30 N in distilled water, (b) 30 N in 0.5 mol/L H_2SO_4, (c) 60 N in distilled water, (d) 60 N in 0.5 mol/L H_2SO_4, (e) 90 N in distilled water, (f) 90 N in 0.5 mol/L H_2SO_4, with frequency 1Hz; (g) EDS of area g, (h) EDS of area h

applied load is up to 90N, the oxide layer becomes thicker, with densification and cracks appearing on the surface.

In 0.5 mol/L sulfuric acid medium, there were obvious grooves and some oxide chips but no oxide films on the wear tracks under applied load of 30N and 60N. With highest applied load of 90N, high deformation and more peelings exist. Besides, some micropores appear on the worn surface. The diameter and number of micropores increased with applied load. This means second phases peeled from the substrate easily under high loading. The mechanism of material removal consists of cutting, ploughing and peeling, inducing considerable mass loss, and plastic removal mechanism changed to brittle removal mechanism with applied load increasing.

3.3 Hardness of the Deformation Layer under the Grinding Surface

The Vickers hardness of cross section under the grinding surface with applied load 90N is illustrated in Fig. 6. According to Hertzian Contact theory, in this study, the minimum Hertzian contact pressure is about 2.8 GPa which is much higher than yield strength of 430 stainless steel. Due to the strong deformation, work hardening occurs, which enhances hardness

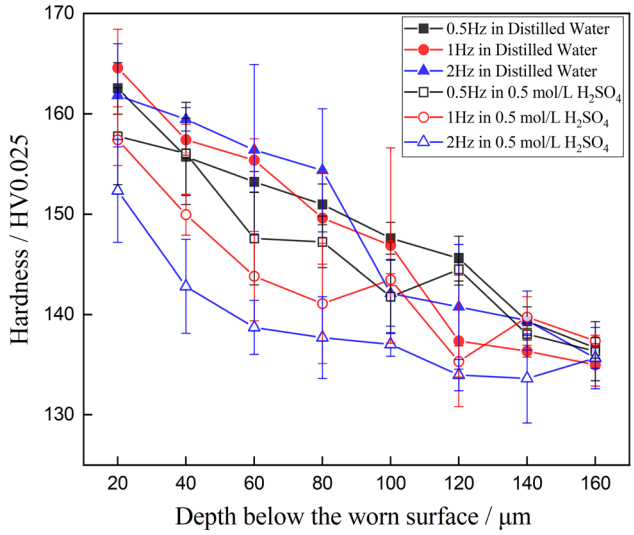

Fig. 6 Cross section Vickers hardness of AISI 430 stainless steel under grinding surface with applied load 90N

of the subsurface. The hardness decreases from the grinding surface to the base material. After grinding, the hardness HV0.025 of AISI 430 is enhanced to 163 near the surface corresponding to the original 135 and the thickness of the deformation layer is about 160 μm. The hardness in 0.5 mol/L sulfuric acid is lower than that in distilled water. Corrosive media results in heterogeneous deformation together with micro cracks and hygrogen, which decreases the mechanical properties of stainless steels (Ref 7, 24, 25) which called hydrogen embrittlement, and pits appear on the worn surface (Ref 26). The influence of frequency on Vickers hardness is similar to that on mass loss. In distilled water, the frequency has little influence on hardness of the cross section, due to the low corrosiveness. While in 0.5 mol/L sulfuric acid, high corrosiveness induced stronger hydrogen embrittlement in long testing duration.

The morphologies of the cross section under the grinding surface are illustrated in Fig. 7. In distilled water (Fig. 7a), it can be seen that close to the surface, friction makes the grains deformed, which brings in work hardening and forms deformation layer. There are some micropores in the deformation layer, which possibly was related to peeling of second phases. High stress caused micro cracks around the second phases, which make them detached. In addition, superficial grains seem to bend toward one direction, which suggests the tendency to align themselves along the direction of the last stroke of the reciprocating sliding (Ref 27). While in 0.5 mol/L sulfuric acid medium, the deformation layer and the deformation of the grains are not obvious under the effect of hydrogen evolution, as shown in Fig. 7(b).

3.4 Interaction Between Wear and Corrosion of AISI 430

Interaction is an important phenomenon for tribocorrosion study. It's related to chemical and mechanical properties of the tribo-pair and tribology interface state including surface or subsurface. Usually, W_{wear} can be measured by wear in media with cathodic protection or corrosion inhibitor (Ref 28-32). While for AISI 430, it has been discussed above that hydrogen has a significant effect on AISI 430. So cathodic protection which may result in hydrogen embrittlement cannot be used in this study. Like Tomlinson did (Ref 32), mass loss in distilled water is considered as W_{wear} in this work. W_{corr} is measured by electrochemical polarization. The interaction and percentage of

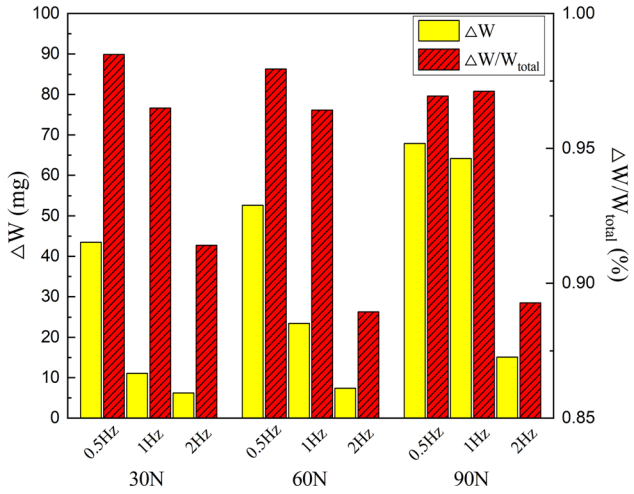

Fig. 8 Mass loss percentage of different parts in tribocorrosion

interaction for different tests are illustrated in Fig. 8. For tribocorrosion of AISI 430 in 0.5 mol/L sulfuric acid medium, interaction between wear and corrosion has great contribution to the mass loss, from 89 to 98%. Both the interaction and proportion of the interaction decrease with the increase in frequency, which means corrosion played an important role during tribocorrosion process under this test condition. On the contrary, both the interaction and proportion of the interaction change a little with the applied load, which means mechanics is second factor under this condition.

3.4.1 Effects of Cathodic Reactions on Tribocorrosion Behaviors. Corrosion process has great effect on tribocorrosion. In this study, anodic reaction is fixed as metal dissolution, $M \rightarrow M^{n+} + ne^{-}$. Different cathodic reactions in different media can change tribocorrosion behavior. In distilled water, the cathodic reaction is oxygen reduction, which makes the surface covered with passive film. During tribocorrosion test, passive films experience the cycle from film removal to film regeneration. On the one hand, combined with oxidation caused by friction, oxide film formed on the wear scar, which has positive effects on corrosion resistance. On the other hand, oxide film with a certain thickness has bearing capacity and improves wear resistance. So, in distilled water, the mass loss

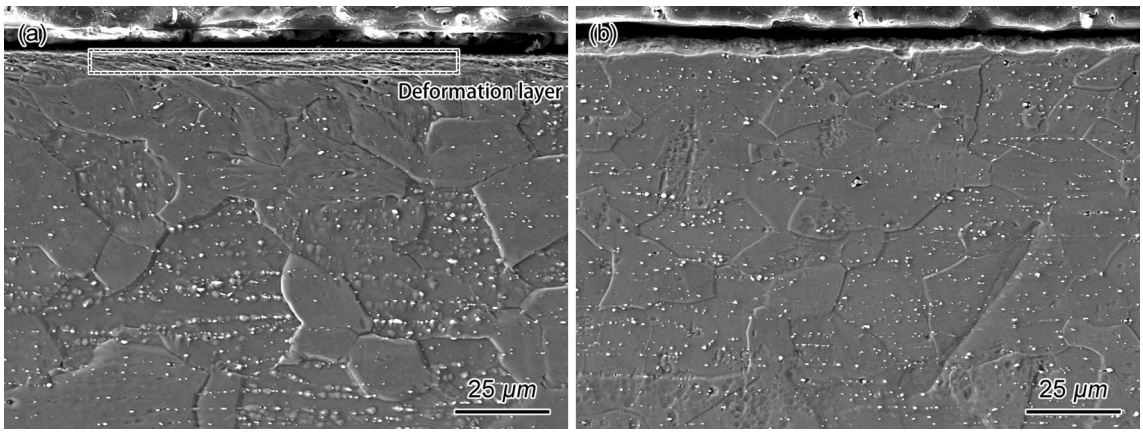

Fig. 7 Cross section morphologies of AISI 430 stainless steel with applied load 90 N, frequency 1 Hz, in (a) distilled water, (b) 0.5 mol/L H_2SO_4

of AISI 430 is less than 2 mg under different loads.

In 0.5 mol/L sulfuric acid medium, the cathodic reaction is hydrogen evolution, which can damage the passive film. Although friction oxidation also exists, oxide film can't be found on the surface due to strong H^+ environment. Furthermore, there are many defects formed on the fresh surface due to the effect of wear, then H^+ invades into materials through these defects, accelerating the corrosion speed. In the wear process, due to the existence of second phase, the difference of elastic modulus between matrix and the second phase causes the mismatch on the interface (Ref 33, 34), together with the hydrogen, leading to initiation and propagation of the micro cracks. The mechanical property degeneration of materials caused by hydrogen is pervasive in stainless steels (Ref 35-39). Therefore, tribocorrosion property of AISI 430 in sulfuric acid medium is worse than that in distilled water, e.g, more mass loss, lower hardness near the surface, indicating the corrosion caused by hydrogen evolution accelerates tribocorrosion.

3.4.2 Effects of Microstructures of Stainless Steels on Tribocorrosion Behaviors. Mechanical and chemical properties of stainless steels are related to microstructures. Work hardening is not obvious in AISI 430. It is well known that ferrite structure cannot occur Twinning Induced Plasticity (TWIP) or Transformation Induced Plasticity (TRIP) phenomena, relative to austenitic stainless steel. So, work hardening of AISI 430, which improves abrasive resistance, is limited and accomplished by impeding the movement of dislocations with second phases (Ref 40). However, the heterogeneous microstructure generates galvanic corrosion. Dispersed cathodic second phases in AISI 430, together with anodic substrates, accelerate the corrosion rate in 0.5 mol/L sulfuric acid, which has disadvantages of anti-tribocorrosion.

Beyond these two points, second phase also plays a bad role in tribocorrosion behavior of AISI 430 in sulfuric acid medium. As mentioned before, hydrogen embrittlement degenerates mechanical properties, especially at the frictional interface. Stress mismatching caused by the second phase, accelerates the immersion of hydrogen, resulting in embrittlement and desquamation. Therefore, AISI 430 has more mass loss during tribocorrosion process in sulfuric acid medium.

3.4.3 A Model for Interaction Between Wear and Corrosion in Tribocorrosion of AISI 430. A model for interaction between wear and corrosion in tribocorrosion of AISI 430 is proposed as Fig. 9. In distilled water, with the intense oxidation, protective oxide layer forms on the worn surface. Meanwhile, high contact stress makes the grains deform and enhances the mechanical properties at the frictional interface. In this condition, H_2O medium lubricates interface and relieves wear. The oxide film formed by electrochemical reaction and friction process is beneficial to anti-tribocorrosion, promoting corrosion resistance and load bearing.

In 0.5 mol/L sulfuric acid, passive film cannot form on the surface. In the tribocorrosion process the fresh surface with many defects induced by wear exposes to H^+ environment. This can accelerate corrosion, promote hydrogen immersion and degenerate mechanical properties. In this condition, interaction worsens tribocorrosion behaviors. Although the friction can harden the subsurface, hydrogen embrittlement makes materials remove easily.

4. Conclusions

(1) In distilled water, the cathodic reaction is oxygen reduction which is in favor of oxide films forming on the surface. While in 0.5 mol/L sulfuric acid medium, hydrogen evolution reaction takes effect. It can restrain the formation of oxide films, induce hydrogen embrittlement, and worsen the tribocorrosion properties.

(2) The wear loss of AISI 430 in water increases with the loading, but shows little change with the reciprocating frequency. The wear mechanism is abrasive wear, including cutting, furrow and plastic deformation. The wear loss of AISI 430 in sulfuric acid increases with the load and decreases with the increase in reciprocating frequency. The wear mechanism is abrasive wear, including cutting and spalling.

(3) The wear loss of 430 in sulfuric acid is much higher than that in distilled water, and there is significant interaction between corrosion and wear, which accounted for 89-99% of the total amount of damage. The effect of frequency on the interaction is more significant than that of load, which means corrosion is primary factor and wear is the second factor under this test conditions.

(4) Microstructure play an important role in tribocorrosion behavior of stainless steel in sulfuric acid. Second phases are benefit to improve abrasive resistance. While

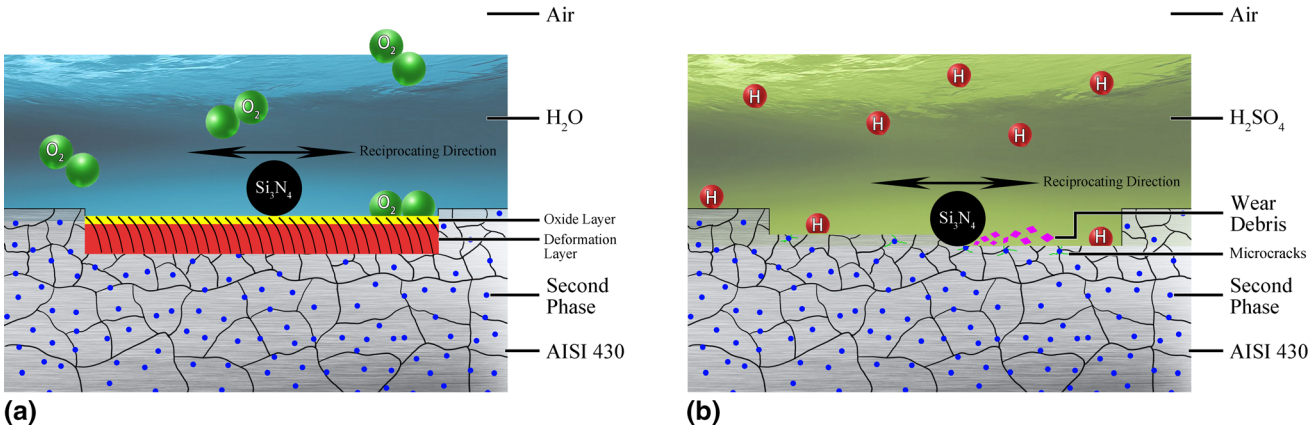

Fig. 9 Tribocorrosion schematic diagram of AISI 430 in (a) distilled water, (b) 0.5 mol/L H_2SO_4

in sulfuric acid medium, it results in galvanic corrosion and worsen tribocorrosion behavior.

References

1. C. Kajdas, E. Wilusz and S. Harvey, *Encyclopedia of Tribology*, Elsevier, 1990
2. B. Hou, X. Li, X. Ma, C. Du, D. Zhang, M. Zheng, W. Xu, D. Lu and F. Ma, The Cost of Corrosion in China, *npj Mater. Degrad.*, 2017, **1**(1), p 1–10
3. K. Holmberg, P. Andersson and A. Erdemir, Global Energy Consumption Due to Friction in Passenger Cars, *Tribol. Int.*, 2012, **47**, p 221–234. (**in English**)
4. Y. Sun and V. Rana, Tribocorrosion Behaviour of AISI 304 Stainless Steel in 0.5 M NaCl Solution, *Mater. Chem. Phys.*, 2011, **129**(1–2), p 138–147. (**in English**)
5. A.C. Vieira, L.A. Rocha, N. Papageorgiou and S. Mischler, Mechanical and Electrochemical Deterioration Mechanisms in the Tribocorrosion of Al Alloys in NaCl and in $NaNO_3$ Solutions, *Corros. Sci.*, 2012, **54**, p 26–35. (**in English**)
6. M. Azzi and J.A. Szpunar, Tribo-Electrochemical Technique for Studying Tribocorrosion Behavior of Biomaterials, *Biomol. Eng.*, 2007, **24**(5), p 443–446. (**in English**)
7. X. Jiang, S. Li and S. Li, *Corrosive Wear of Metals*, Chemistry Industry Press, Beijing, 2003
8. R.A. Lula, *Stainless Steel*, American Society for Metals, 1986
9. G. Tammann, The Chemical and Galvanic Characteristics of Compound Crystals and their Atomic Distribution: An Article on the Understanding of Alloying, *Z. Anorg. Allg. Chem.*, 1919, **107**(1/3), p 1–239. (**in German**)
10. H. Fischmeister and U. Roll, Passive Layers on Stainless-Steels: A Survey of Surface-Analysis Results, *Fresenius Zeitschrift Fur Analytische Chemie*, 1984, **319**(6–7), p 639–645. (**in German**)
11. J. Beddoes and J.G. Parr, *Introduction to Stainless Steels*, ASM International, 1999
12. T. Hong, T. Ogushi and M. Nagumo, Effect of Chromium Enrichment in the Film Formed By Surface Treatments on the Corrosion Resistance of Type 430 Stainless Steel, *Corros. Sci.*, 1996, **38**(6), p 881–888. (**in English**)
13. I. Sekine, S. Hatakeyama and Y. Nakazawa, Corrosion Behavior of Type-430 Stainless-Steel in Formic and Acetic-Acids, *Corros. Sci.*, 1987, **27**(3), p 275–288. (**in English**)
14. R. Nishimura, D. Shiraishi and Y. Maeda, Hydrogen Permeation and Corrosion Behavior of High Strength Steel MCM 430 in Cyclic Wet-Dry SO2 Environment, *Corros. Sci.*, 2004, **46**(1), p 225–243. (**in English**)
15. S. Hastuty, A. Nishikata and T. Tsuru, Pitting Corrosion of Type 430 Stainless Steel under Chloride Solution Droplet, *Corros. Sci.*, 2010, **52**(6), p 2035–2043. (**in English**)
16. R.M. Fisher, E.J. Dulis and K.G. Carroll, Identification of the Precipitate Accompanying 885-Degrees-F Embrittlement in Chromium Steels, *Trans. Am. Inst. Mining Metall. Eng.*, 1953, **197**(5), p 690–695. (**in English**)
17. M.J. Blackburn and J. Nutting, Metallography of Iron-21 Per Cent Chromium Alloy Subjected to 457 Degrees C Embrittlement, *J. Iron Steel Inst.*, 1964, **202**(7), p 610–613. (**in English**)
18. M. Liu, D.L. Duan, S.L. Jiang, M.Y. Li and S. Li, Tribocorrosion Behavior of 304 Stainless Steel in 0.5 mol/L Sulfuric Acid, Acta Metall, *Sin.-Engl. Lett.*, 2018, **31**(10), p 1049–1058. (**in English**)
19. C. Wagner and W.E. Traud, The Analysis of Corrosion Procedures through the Interaction of Electrochemical Partial Procedures and on the Potential Difference of Mixed Electrodes, *Z. Elektrochem. Angew. Phys. Chem.*, 1938, **44**, p 391–402. (**in German**)
20. Y.X. Qiao, Y.G. Zheng, P.C. Okafor and W. Ke, Electrochemical Behaviour of High nitrogen Bearing stainless Steel in Acidic Chloride Solution: Effects of Oxygen, Acid Concentration and Surface Roughness, *Electrochim. Acta*, 2009, **54**(8), p 2298–2304. (**in English**)
21. L. Bjornkvist and I. Olefjord, The Electrochemistry of Chromium in Acidic Chloride Solutions: Anodic-Dissolution and Passivation, *Corros. Sci.*, 1991, **32**(2), p 231–242
22. R. Iler, *The Chemistry of Silica*, Wiley, New York, 1979
23. N. Liu, J.Z. Wang, B.B. Chen and F.Y. Yan, Tribochemical Aspects of Silicon Nitride Ceramic Sliding Against Stainless Steel under the Lubrication of Seawater, *Tribol. Int.*, 2013, **61**, p 205–213. (**in English**)
24. J.R. Jiang and M.M. Stack, Modelling Sliding Wear: From Dry to Wet Environments, *Wear*, 2006, **261**(9), p 954–965. (**in English**)
25. J. Jiang, M.M. Stack and A. Neville, Modelling the Tribo-Corrosion Interaction in Aqueous Sliding Conditions, *Tribol. Int.*, 2002, **35**(10), p 669–679. (**in English**)
26. S. Zor, M. Soncu and L. Capana, Corrosion Behavior of G-X CrNiMoNb 18–10 Austenitic Stainless Steel in Acidic Solutions, *J. Alloy. Compd.*, 2009, **480**(2), p 885–888. (**in English**)
27. J. Perret, E. Boehm-Courjault, M. Cantoni, S. Mischler, A. Beaudouin, W. Chitty and J.P. Vernot, EBSD, SEM and FIB Characterisation of Subsurface Deformation During Tribocorrosion of Stainless Steel in Sulphuric Acid, *Wear*, 2010, **269**(5–6), p 383–393. (**in English**)
28. W. Schumacher, Corrosive Wear Synergy of Alloy and Stainless Steel, *Wear Mater.*, 1985, **1985**, p 558–566
29. T.C. Zhang, X.X. Jiang, S.Z. Li and X.C. Lu, A Quantitative Estimation of the Synergy Between Corrosion and Abrasion, *Corros. Sci.*, 1994, **36**(12), p 1953–1962. (**in English**)
30. H. Abdelkader and S.M. Elraghy, Wear-Corrosion Mechanism of Stainless-Steel in Chloride Media, *Corros. Sci.*, 1986, **26**(8), p 647–653. (**in English**)
31. S.M. Elraghy, H. Abdelkader and M.E. Abouelhassan, Electrochemistry of Abrasion Corrosion of Low-Alloy Steel in 1-Percent Nacl Solution, *Corrosion*, 1984, **40**(2), p 60–61. (**in English**)
32. W.J. Tomlinson and M.G. Talks, Erosion and Corrosion of Cast-Iron under Cavitation Conditions, *Tribol. Int.*, 1991, **24**(2), p 67–75. (**in English**)
33. U.K. Viswanathan, G.K. Dey and M.K. Asundi, Precipitation Hardening in 350-Grade Maraging-Steel, *Metall. Trans. Phys. Metall. Mater. Sci.*, 1993, **24**(11), p 2429–2442. (**in English**)
34. S.W. Ooi, P. Hill, M. Rawson and H. Bhadeshia, Effect of Retained Austenite and High Temperature Laves Phase on the Work Hardening of an Experimental Maraging Steel, *Mater. Sci. Eng. Struct. Mater. Prop. Microstruct. Process.*, 2013, **564**, p 485–492. (**in English**)
35. V. Olden, C. Thaulow and R. Johnsen, Modelling of Hydrogen Diffusion and Hydrogen Induced Cracking in Supermartensitic and Duplex Stainless Steels, *Mater. Des.*, 2008, **29**(10), p 1934–1948. (**in English**)
36. R.G. Davies, Hydrogen Embrittlement of Dual-Phase Steels, *Metall. Trans. Phys. Metall. Mater. Sci.*, 1981, **12**(9), p 1667–1672. (**in English**)
37. A.W. Thompson and J.A. Brooks, Hydrogen Performance of Precipitation-Strengthened Stainless-Steels Based on a-286, *Metall. Trans. Phys. Metall. Mater. Sci.*, 1975, **6**(7), p 1431–1442. (**in English**)
38. T. Neeraj, R. Srinivasan and J. Li, Hydrogen Embrittlement of Ferritic Steels: Observations On Deformation Microstructure, Nanoscale Dimples and Failure by Nanovoiding, *Acta Mater.*, 2012, **60**(13–14), p 5160–5171. (**in English**)
39. M.L. Holzworth, Hydrogen Embrittlement of Type 304L Stainless Steel, *Corrosion*, 1969, **25**(3), p 107–115. (**in English**)
40. A.J. Ardell, Precipitation Hardening, *Metall. Trans. Phys. Metall. Mater. Sci.*, 1985, **16**(12), p 2131–2165. (**in English**)